

# Detection and Classification of Brain tumors using Deep Learning and Compressive Sensing in magnetic resonance imaging

## Detección y clasificación de tumores cerebrales mediante Deep Learning y Compressive Sensing en resonancia magnética

<sup>a</sup>William Suárez-Jaimes, <sup>b</sup>Luis Enrique Mendoza, <sup>c</sup>Leonor Jaimes-Cerveleón, <sup>d</sup>Zulmary Nieto-Sánchez

-  a. Ingeniero en Telecomunicaciones, William.suarez@unipamplona.edu.co, Universidad de Pamplona, Pamplona, Colombia.
-  b. Magister en Ingeniería Biomédica, Luis.mendoza@unipamplona.edu.co, Universidad de Pamplona, Pamplona, Colombia.
-  c. Magister en Administración de Empresas e Innovación, Leonor.cerveleon@unipamplona.edu.co, Universidad de Pamplona, Pamplona, Colombia.
-  d. Doctora en Educación, zulmarycarolinanisa@ufps.edu.co, Universidad Francisco de Paula Santander, Cúcuta, Colombia

Recibido: Junio 1 de 2021 Aceptado: Octubre 8 de 2021

**Forma de citar:** Forma de citar: W. Suárez-Jaimes, L.E. Mendoza, L. Jaimes-Cerveleón, Z. Nieto-Sánchez “Detection and Classification of Brain tumors using Deep Learning and Compressive Sensing in magnetic resonance imaging”, *Mundo Fesc*, vol. 11, S4, pp. 40-55, 2021

### Abstract

---

In this article he presents a new methodology for the detection of brain tumors in magnetic resonance imaging. The FIGSHARE database of the University of Southern Medicine, Guangzhou, China, was used. Mathematical morphology techniques were used for image conditioning to detect the area of interest in the image. Additionally, an algorithm was developed to determine the type of slice (axial, sagittal or coronal). For this procedure, the statistical mathematical technique k-means was used. Likewise, a pattern extraction was performed from each image using compressive sensing (CS). For the detection, segmentation and classification of the tumors, Deep learning based on convolutional neuronal networks was implemented applying R-CNN (regions with convolutional networks). The results obtained in the validation stage achieved a classification and detection of brain tumors in magnetic resonance images with high percentages of accuracy of 87.5% and 95.2%. The data was divided into 65% for network training, 18% for the test and 17% for the validation process. Finally, by applying deep learning and compressive sensing, brain tumors were detected and classified into three different types: meningioma, glioma, and pituitary with an accuracy rate of 87.5% and 95.2%.

**Keywords:** Compressive sensing, Deep learning, magnetic resonance imaging, image classification, convolutional neural network, brain tumors.

---

**Autor para correspondencia:**

\*Correo electrónico: Luis.mendoza@unipamplona.edu.co



## Resumen

---

En este artículo presenta una nueva metodología para la detección de tumores cerebrales en imágenes de resonancia magnética. Se utilizó la base de datos FIGSHARE de la Universidad de Medicina del Sur, Guangzhou, China. Se utilizaron técnicas de morfología matemática para el acondicionamiento de la imagen con el fin de detectar el área de interés en la imagen. Además, se desarrolló un algoritmo para determinar el tipo de corte (axial, sagital o coronal). Para este procedimiento se utilizó la técnica matemática estadística k-means. Asimismo, se realizó una extracción de patrones a partir de cada imagen utilizando la técnica de detección compresiva (CS). Para la detección, segmentación y clasificación de los tumores se implementó el aprendizaje profundo basado en redes neuronales convolucionales aplicando R-CNN (regiones con redes convolucionales). Los resultados obtenidos en la etapa de validación lograron una clasificación y detección de tumores cerebrales en imágenes de resonancia magnética con altos porcentajes de precisión del 87,5% y 95,2%. Los datos se dividieron en un 65% para el entrenamiento de la red, un 18% para la prueba y un 17% para el proceso de validación. Finalmente, aplicando deep learning y compressive sensing, se detectaron y clasificaron los tumores cerebrales en tres tipos diferentes: meningioma, glioma y pituitaria con un porcentaje de precisión del 87,5% y 95,2%.

**Palabras clave:** Sensación compresiva, aprendizaje profundo, imágenes de resonancia magnética, clasificación de imágenes, red neuronal convolucional, tumores cerebrales.

## Introduction

Currently one of the causes that produces a higher percentage of death in humans are malignant tumors or also known as cancer, such tumors can occur in the body and move to the brain better known as secondary and can also occur directly in the brain called primary. These tumors are now classified into families and types and are named according to where they originate. For these reasons, this article focuses on the MRI analysis of brain tumors known as meningiomas, gliomas, and pituitary tumors, where meningiomas arise from the meninges, which are membranes that cover the brain and spinal cord, gliomas that arise in the brain and spinal cord, they begin in the glial cells that surround the nerve cells, and pituitary tumors that originate significantly in the cells of the pituitary itself located in the bony space called the sella at the base of the skull. Such affectations are observed in medicine by means of computerized tomography images, magnetic resonance, x-rays, among others. These types of images currently show a medical representation in gray levels of various contexts such as heart,

brain, lung, abdomen, lumbar, pelvic and various parts of the human body. On the other hand, the processing of signals and images has been evolving in an important way to the point of being one of the biggest advances in the field of medicine in such a way that mathematical processing techniques have been included in the analysis of medical images in order to obtain much more precise results allowing the specialist to have more reliable and quicker conclusions at the time of a clinical diagnosis. Different works have been carried out through time, for the classification and segmentation of brain tumors in magnetic resonance images [1-2], works in which traditional processing techniques were used such as discrete cosine transformation, segmentation through Fuzzy media, extraction using areas and circularity, giving as a major result the improvement of processing capacity, high speed in computational requirements. On the other hand, the works [3-8] have achieved important results using deep neural networks, wavelet transform, vector support machines, convolutional neural networks, anisotropic filtering,

k-means and among other techniques for the classification of tumors such as glioma, sarcoma, glioblastoma or if they are only benign or malignant are in, the results show percentages of accuracy of 95%, 80% to 90%, 96.05%, 83%, 96.97%, 88% respectively. Other relevant works were performed by Sofiane Tchoketch Kebir, Slimane Mekaoui [9], SM Kamrul Hasan; Cristian A. Linte [10], Pradeep Kumar Mallick et al. [11], these authors show that fusing convolutional neural networks and deep learning together with pre-processing and post-processing techniques can improve the percentages of classification, segmentation and processing speed. These papers show accuracy results of 95%, 98% respectively. It is also important to note that no report has been found that shows the use of CS as a pattern extraction method in magnetic resonance

imaging for tumor detection. CS is a novel compression method which is evaluated and compared in several works, such as [12-13], where high performance of the technique in compression and reconstruction of images is obtained. Unlike the works mentioned above, this article is based on the use of compressive sensing for pattern extraction and classification by deep neural networks.

## Materials and methods

### Database acquisition

The FIGSHARE [14] database was used, MRI images of size 512 x 512 in grayscale. It was divided into 65% for training, 18% for testing and 17% for validation. Figure 1 shows the types of slices found on an axia, coronal and sagittal brain MRI.

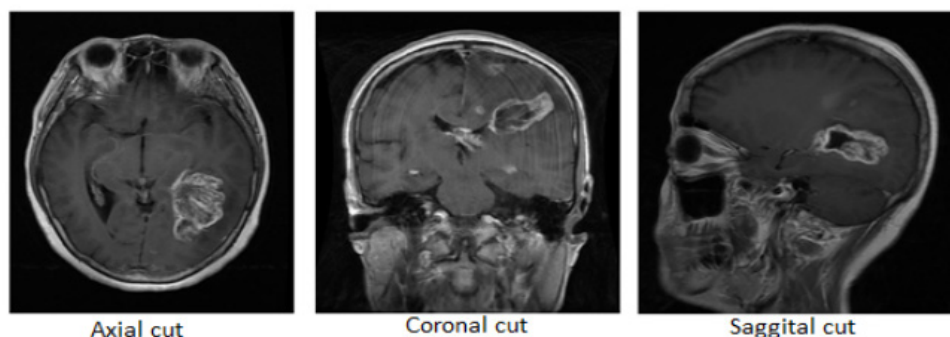


**Fig. 1.** Types of cuts in database images. Autor: [FIGSHARE](#) [14]

Images of 3 types were used showing 3 classes of glioma, meningioma and pituitary tumors, resulting in 3 categories to be classified and 1 background category. In this article k-means was used to classify the type of image or image slice, in addition CS was used for pattern extraction and Deep learning was used for classification. These techniques are described below.

### K-means

K-means is an unsupervised grouping method, where groups of data are created

from the calculation of the closest distance. This method works by creating random centroids and calculating the distances between the data. Each group is labeled according to the number of groups desired [15]. Equation 1 shows the distance calculation used to make the clusters. Finally, the calculated centroids were used to find the slice of the image.

$$distance = \sqrt{(x1-x2)^2 + (y1-y2)^2} \quad (1)$$

Where  $x, y$  are coordinates of the Cartesian plane.

To train the grouping, the central row, the central column, and the main and secondary diagonals of 15 images, 5 from each cut, were taken as a reference (pattern). For the classification, the centroids generated for each type were saved and in its validation the pattern of each image was subtracted, where the nearest distance value shows the type of cut.

**Compressive sensing**

Compressive sensing is a novel compression technique in which the most important thing is to significantly reduce the number of samples for the reconstruction of a signal.

Compressive sensing states that an image can be reconstructed with high probability if the signal is in a low density form but it must always meet two important guidelines which are that of scarcity in any domain and at the same time that it is inconsistent based on the measurement matrix. This leads to break the Shanon/Nyquist theorem that says that to reconstruct a signal you need twice the frequency of the signal, compressive sensing works by multiplying a sparse vector by a random matrix called a dictionary where as a result it gives a vector of size equal to the number of rows in the dictionary, this process is clearly shown in the following figure 2. [16].

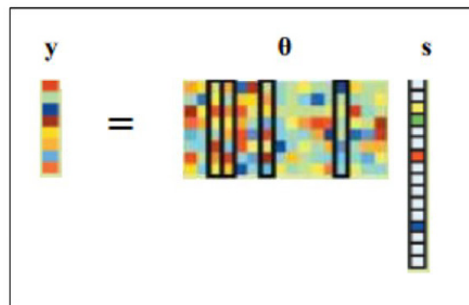


Figura 2. Compressive sensing process where S is the vector sparse and  $\theta$  is the dictionary

The sparse signal was obtained using discrete 2D cosine transform, it is highlighted that there are other techniques such as wavelet and Fourier. Below is an example of a sparse signal in the discrete cosine domain see figure 3. Note how most of its values are very close to its baseline and few values have an amplitude with significant values.

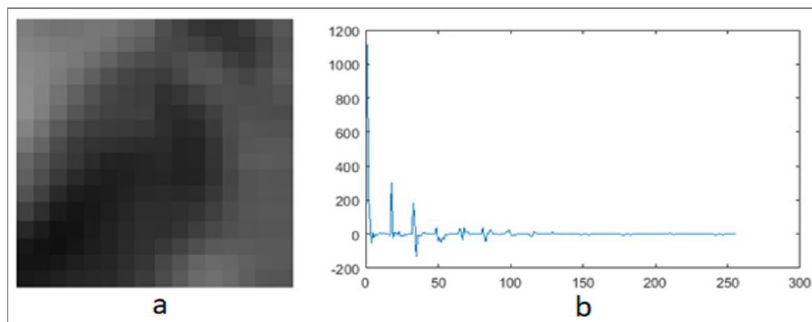


Figura 3. (a). 16x16 cropped image of the original image, vector sparse of image (a) from the cosine transform.

Mathematically compressive sensing is expressed in the following equation:

$$Y = \Phi * V_s \quad (2)$$

Where:  $Y = \text{compressed signal} = \text{dictionary matrix } Vs = \text{vector sparse}$

In CS the dictionary must meet the following criteria:

- The matrix must be random, orthogonal and orthonormal.
- The rows of the matrix must be much smaller than the columns of the matrix  $f \ll c$ .

The number of rows is calculated in equation (3). In this article  $f=64$ .

$$f = K \log(n) * c \quad (3)$$

Where:  $f = \text{number of rows}$ ,  $K = \text{number of peaks in the vector}$ ,  $n = \text{length of the sparse vector}$  and  $c = \text{constant is usually taken as 1}$ .

- The columns of the matrix must be equal to the value of the length of the sparse vector.
- The isometric constraint property given by equation 4 below must be met.

$$|Vs|_2^2(1 - \delta s) < |\Phi Vs|_2^2 < |Vs|_2^2(1 + \delta s) \quad (4)$$

Where:  $\delta s = \text{isometric restriction constant}$ , have values of 0 and 1. And is applied the norm  $L_2$ .

In this paper, compressive sensing was used as a pattern extraction. This process was carried out by taking each magnetic resonance image and dividing it into  $16 \times 16$  size images. Discrete cosine transformation was applied to each small image in order to obtain a sparse signal. Once the sparse image is obtained, the result is vectorized. On the other hand, for the creation of the dictionary, an orthogonal random matrix was used where the values were re-scaled from 1 to 255, the size of the dictionary is  $64 \times 256$ , then from the compressed vectors a

new image was generated, where a pattern image of the original image is reflected but of smaller size. These pattern images were used to train the convoluted neural network.

### Deep learning

Deep learning is also known as deep neural networks, is a branch of machine learning, uses an automated form based on predictive analysis and probability, such networks are able to learn with respect to the input-output relationship, this is done thanks to a high amount of data as examples. Deep learning uses what it learns to create a statistical model as an output with a highly acceptable accuracy, for the classification of any object. Deep learning because it is a deep neural network uses neural networks, where the inputs are multiplied by initial weights that are generally random and are updated from the cycles that are generated, this process results in an output which is described with the following equation.

$$Y = F(\sum_{i=0}^n w_i * x_i) \quad (5)$$

Where:  $F = \text{activation function}$ ,  $n = \text{input number}$ ,  $w = \text{weights}$  and  $x = \text{inputs}$

Deep learning is practically a technique created for the analysis of images and in the case of medical images its use is relevant since it uses layered feature detectors as shown in the following figure4, each. [17]. Note how in this type of network its structure is divided into input, feature extraction and classification where the input is a conditioning layer of the image to be processed such as the change of size or clipping of the region of interest, feature extraction consists of convolution and pooling processes that seek to extract relevant features from each image that is being used and classification of fullconnected processes in order to connect all the features extracted with the labels.

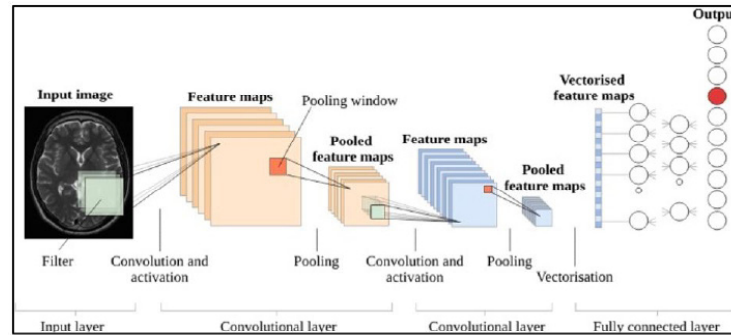


Figure 4. Process of a deep neural network. Alexander Selvikvåg Lundervold, Arvid Lundervold. [17]

In this paper we used a pre-trained network called R-CNN which is a convolutional neural network that works with regions where the image is entered by tagging the object region and in which the CNN automatically cuts out the image region, resizes it, and the CNN classifies the proposed cut-out regions. This deep neural network consists of 15 layers that are divided into input sections (ImageInputLayer), feature extraction section (Convolution2DLayer, MaxPooling2D, ReLuLayer, veragePooling2DLayer) and the classification section (FullConnectedLayer, SoftmaxLayer, ClassificationOutputLayer). [17]. The use of the convoluted network is explained below.

### 1) Input section

This layer is responsible for taking the image, cropping the labeled region on the image, and resizing and normalizing it for feature extraction. In this article the images were resized to 32x32x3.

### 2) Feature extraction section

The first layer is the Convolution which filters the image using different masks of different sizes that move through the image in the form of a sliding window. In this article we used convolution layers with 5x5 masks with a number of filters of 32. This convolution is governed by the following equation [18-27].

$$s(i,j) = (I * K)(i,j) = \sum_m \sum_n I(m,n) K(i-m,j-n) \quad (6)$$

Where:  $m$  and  $n$  are the rows and columns of the image,  $(i, j)$  indicate the kernel shift  $K=i$  is the kernel to be used and  $I$ = original image

Pooling is the image reduction layer without altering the image depth, it can be presented in different types, it can be maxPooling that consists in passing a mask through the image of different sizes in the form of a sliding window and it reduces the size of the image by calculating the higher transition value, it can also be averagePooling that works in the same way as maxPooling only that it does not calculate the higher number but the average of each mask. We used 1 maxPooling and 2 averagePooling of 3x3 masks. Also, ReLU is a non-linear trigger function that behaves in the way that if values are greater than or equal to zero it leaves them equal and if values are less than zero it cancels them out leaving only positive values, its behavior is described in the following equation 7 [27-32].

$$f(x) = \begin{cases} 0 & \text{si } x < 0 \\ x & \text{si } x \geq 0 \end{cases} \quad (7)$$

in this work, 4 ReLU activation layers were used, 3 in the convolution outputs and one for the fullconnected layer.

### 3) Classification section

FullConected is a fully connected layer in which it combines all the features learned in the previous layers in order to identify the highest percentages. Here 2 layers of fullconnected were used, one to combine the characteristics of the convolutions, another to combine the characteristics of the last extraction layer with the number of categories to be classified, in this case 4 background, glioma tumor, meningioma tumor, pituitary tumor. Softmax is also known as exponential function where it calculates percentages for each category, to improve classification problems. In this work a softmax function was used before the classification layer. Classification determines which category the input image belongs to based on the percentages provided by the softmax layer. The softmax function

is described in Equation 8 [33-38].

$$\frac{e^Y_j}{\sum_{k=1}^K (e^Y_k)} \quad (8)$$

Where:  $Y$ = Output of hidden layers and  $K$ =Number of model classes

The implemented network had changes like the number of categories in the classification layer and the number of outputs in the fullconnected layer from a value of two categories to 4 and from 2 inputs to 4, thus changing the initial weights in the classification layer. For the training, a region tagging was performed in which the images were loaded and tagged for each type of tumor to later enter the data. This process was done for the normal images and for the CS standard images, as shown in figure 5 [39-41].

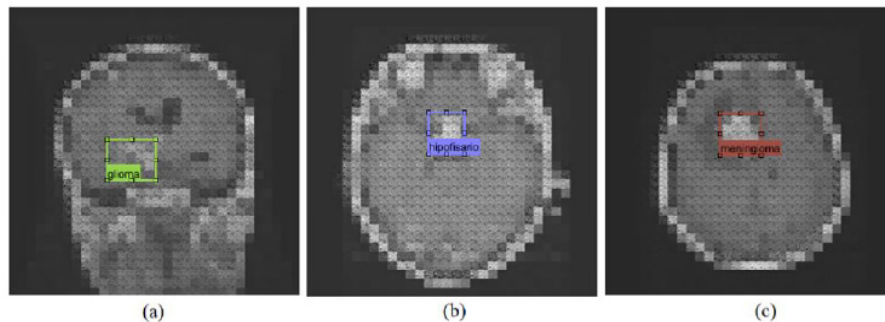


Fig. 5. Image Labeler labelling, (a) green labelling for glioma class tumours, (b) blue labelling for pituitary class tumours, (c) brown labelling for meningioma class tumours.

The neural network training process was performed using 4921 images and had a computerized training cost of 35 hours.

### Results

The results are shown in relation to each stage carried out during the research. As a first result the cut classification based on the K-means function is shown, as a second the extraction of patterns from CS, and as a third the results of segmentation and classification of tumors using the original image and using the CS patterns.

In the first stage the cut type classification was evaluated using the k-means technique where it results in a 97% accuracy rate. In the classification process it was observed that the axial slice images presented similarities in both coronal and sagittal slice, while the sagittal and coronal slice images were different which led to the application of an averaging technique that determined if the image was axial slice. Figure 6 shows the classification of the three types of cuts.

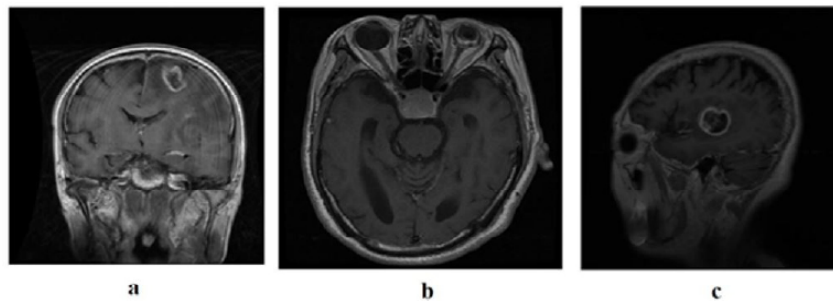


Fig. 6. Classification cut, a) coronal cut, b) axial cut, c) sagittal cut

In the pattern extraction, where it was determined which image cutout size was best suited for the pattern extraction, from it the type of dictionary to use was determined giving as best result the use of 16x16 cutouts in the images and 8x8 in the pattern extraction reducing the image by 1/4, with a 64x256 dictionary. Figure 7 shows the different clipping sizes used.

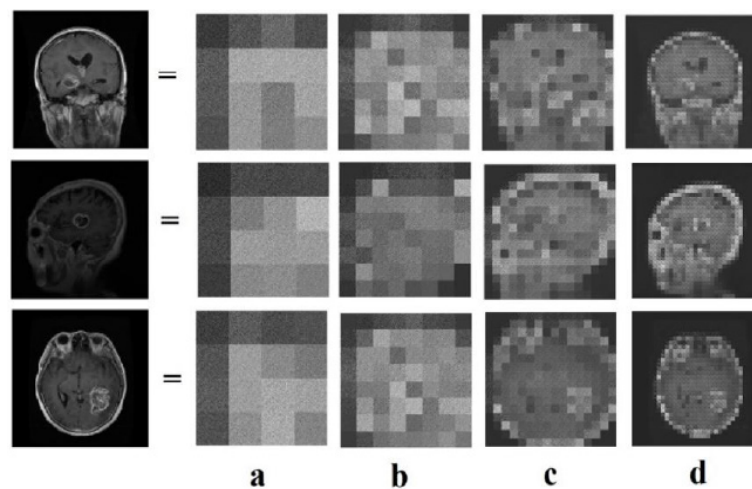


Fig. 7. Original image after different degrees of CS, a) 128x128 clipping dictionary 4096x16384, b) 64x64 clipping dictionary 1024x4096, c) 32x32 clipping dictionary 256x1024, d) 16x16 clipping dictionary 64x256

Note how from the dictionary size onwards important features are kept or removed in the image. In this article the image d was selected as the best result, because the tumor area can be seen more clearly, this resulted in working with a dictionary of random values from 0 to 255, and a size of 64x256. On the other hand, figure.8 shows the detail applying CS in different cuts together with a manual segmentation used to train the convolutional network, here we can appreciate the different patterns in each type of tumor. Note that tumors have different shapes and morphological characteristics, which makes the classification process complex, regardless of whether it is the same type of tumor in the same type of cut. This process was performed on 118 images.

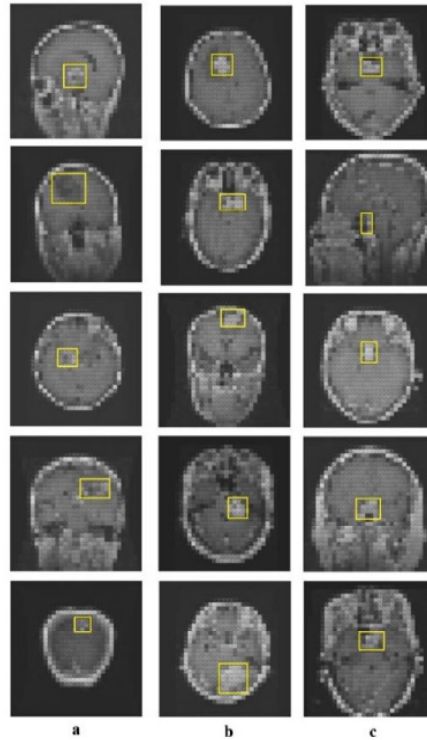


Fig. 8. CS tumor segmentation, a) glioma, b) meningioma, c) pituitary

Finally, the segmentation and classification of brain tumors was performed using CS and original image giving classification and segmentation results in each case shown in the following tables.

Table I. Percentages of segmentation and classification

Training with CS		
Tumor type	Percentage Segmentation	Clasification percentage
glioma	87,32%	90,14%
meningioma	81,39%	90,6%
Hipofisario	92,85%	90,17%
<b>Total</b>	<b>87,18%</b>	<b>90,30%</b>
Training with original imagen		
Tumor type	Percentage Segmentation	Clasification percentage
glioma	76%	80,20%
meningioma	87%	74,35%
Hipofisario	79,22%	78,13%
<b>Total</b>	<b>80,74%</b>	<b>77,56%</b>

In table I, the training results are shown in terms of classification and segmentation of the tumor. Note that the most relevant results are using CS as characteristic patterns with 92.85% for pituitary tumor segmentation and 90.6% for pituitary tumor classification. These percentages show that

CS can be used as a technique for pattern extraction. It is important to emphasize that the value of the results is due to the fact that not all tumors are the same for a specific category, which makes it difficult for the neuronal network to learn easily and therefore tends to make mistakes.

Table II. Percentages of segmentation and classification

Test with CS		
Tumor type	Percentage Segmentation	Clasification percentage
glioma	72%	72%
meningioma	95,2%	85,7%
Hipofisario	92%	80%
<b>Total</b>	<b>86,4%</b>	<b>79,23%</b>
Test with original image		
Tumor type	Segmentation percentage	Clasification percentage
glioma	46.42%	53.57%
meningioma	60%	55%
Hipofisario	57.69%	65.38%
<b>Total</b>	<b>54,7%</b>	<b>57,98%</b>

The Table II, shows the results of the applied test. A test for the CS space and a test for processing in original images were used. Note that the best results are in the CS space. With 95.2% for segmenting meningioma and with 85.7% for classifying meningiomas. These results confirm that the size and the values selected from the dictionary are the most appropriate to perform a process of segmentation and classification of tumors in magnetic resonance imaging. Here, in relation to false positives and false negatives, we found that there are no false negatives in the results. However, the false positives were 5 images, from the validation and test process. That is to say that 7.9%

of the images had false positives. It is important to mention that this percentage of false positives was obtained from the images with tumors 3 Glioma and 2 Meningioma. Of Pituitary there are no false positives.

According to the average training and test data, CS has a better segmentation than from the original image, it is also shown that CS classification is better than from the original image. This is shown in figure 9 where it can be seen that the CS classification and segmentation is around 80% to 92%, and from the original image it is around 60% to 75%.

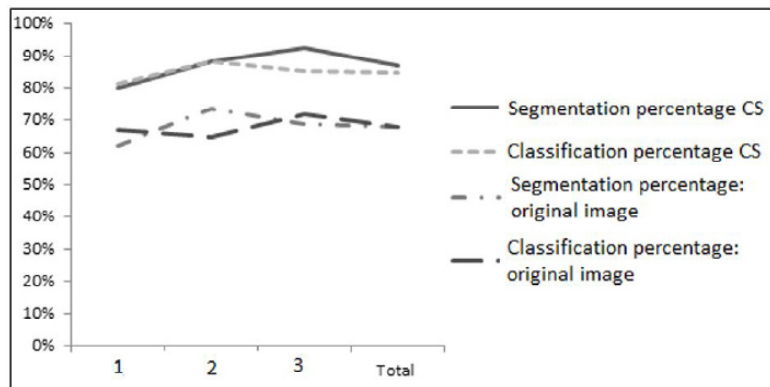


Fig. 9. Classification and segmentation percentages. 1 Glioma. 2 Meningioma. 3. Pituitary

Finally, figure 10 shows the final result of segmentation and classification of the system and processing implemented. These images were not used for training and the system was able to segment or identify the tumor and also classify the type of tumor in each image.

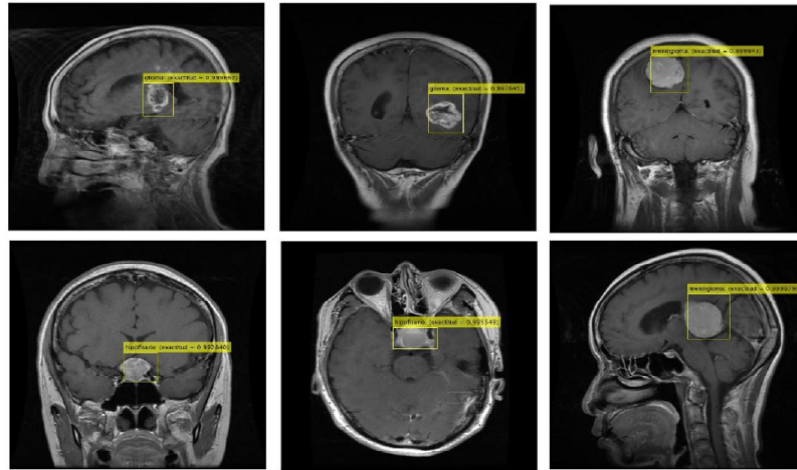


Fig. 10. Final result of classification and segmentation

### *Signal to Noise Ratio*

An analysis was made of how much noise the deep neural network supported so that it would stop working and not detect and classify the tumor. The results showed that the network supports a maximum of 0.013 aggregated white point noise in the image, which means that for the detection of brain tumors in MRI using deep learning and compressive sensing techniques, the system supports a maximum signal-to-noise ratio of 1.3%. Figure.11 shows the classification of different tumors using a signal-to-noise ratio of 1.3%.

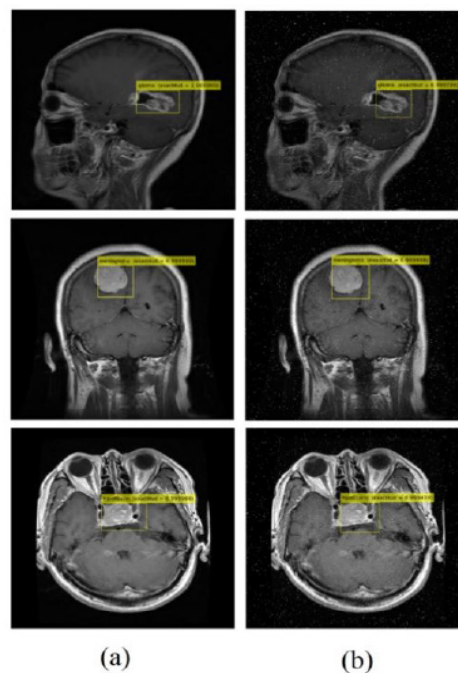


Fig. 11. (a) images without noise detection and classification, (b) images with 1.13% noise detection and classification

### Classification Robustness

A network robustness analysis was performed by implementing image distortion tests in certain percentages, using a pro-media filter which distorted the image in certain percentages according to the size of the kernel. The result was that the image allows for maximum distortions of 13.72% of the number of pixels in the image, so that the system can no longer detect and classify efficiently. It should be noted that the maximum distortion of 13.72% depends on the type of image since there are images that are more difficult to classify by their gray level, by their tumor size, by having areas with similarities to tumors and other factors. Figure.12 shows the classification of distorted images compared to the original image that support various percentages of distortion.

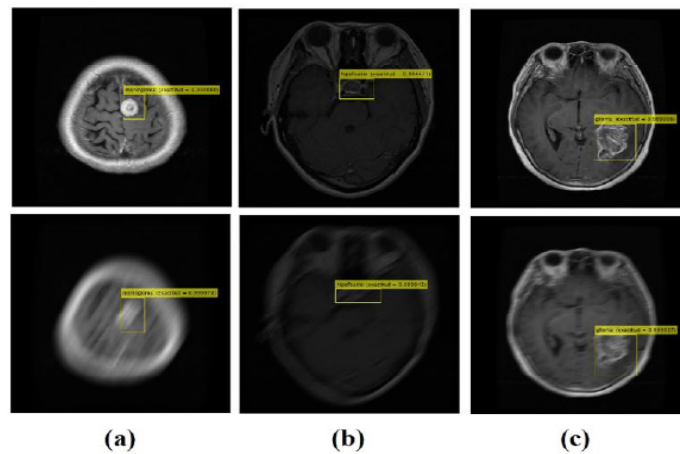


Fig.12. (a) classification with maximum distortion of 13.72%. (b) classification with maximum distortion of 13%. (c) rating with maximum distortion of 7.85%.

### Conclusions and discussion

With the methodology proposed, we were able to classify and segment the types of tumors in an efficient way using novel techniques such as compressive sensing and deep learning, giving as a result that CS can be used for the extraction of patterns in images since it generates different patterns for each type of image. As for the classification of brain tumors using CS, it should be taken into account that at the time of preparing the dictionary, this dictionary should not have opening values since it is impossible for neural networks to detect positive and negative regions at the time of training. Likewise, in the extraction of patterns in a brain MRI with CS works better extracting patterns in small pieces of

image than in the complete image or very large cuts. It has also been shown that a single dictionary can extract patterns on different brain MRIs. Regarding the CS classification compared to the original image classification, it was obtained that the classification and segmentation using compressive sensing is better than the classification and segmentation of the network with the original or raw image since the percentages obtained were higher in CS than with the original image when evaluating in images with which the network has not been trained. As for the robustness and support of the network in brain MRI images, the network has a maximum percentage of 1.3% support for white-spot noise and a maximum percentage of 13.72% support for distortion, making the network

more reliable when entering a brain image with distortion or noise. On the other hand, when obtaining a classification of objects with high percentages, it is necessary to work with high databases since the greater the number of data to train the network, the greater the percentage of accuracy. In the same way, working with high amounts of databases at the time of training a network is recommended to work with GPUs since the processing of neural networks is quite expensive and in normal equipment it can take long times. Finally, for future work, the classification of a larger number of types of tumors is proposed, as well as the classification of the grade of the tumor, since from the grade that the tumor has it is possible to say if the tumor is benign or malignant and also to facilitate the medical diagnosis. The improvement of the network in terms of noise support is also proposed, since the percentage obtained is not very high.

## References

- [1] D. Sridhar and I. Murali Krishna, "Brain Tumor Classification using Discrete Cosine Transform and Probabilistic Neural Network," 2013 International Conference on Signal Processing, Image Processing & Pattern Recognition, Coimbatore, 2013, pp. 92-96.
- [2] A. Sehgal, S. Goel, P. Mangipudi, A. Mehra and D. Tyagi, "Automatic brain tumor segmentation and extraction in MR images," 2016 *Conference on Advances in Signal Processing (CASP)*, Pune, 2016, pp. 104-107
- [3] R. Liu, L.O Hall, D.B. Goldgof, M. Zhou, R.A Gatenby and K.B. Ahmed, "Exploring deep features from brain tumor magnetic resonance images via transfer learning," 2016 *International Joint Conference on Neural Networks (IJCNN)*, Vancouver, BC, 2016, pp. 235-242
- [4] S. Kumar, C. Dabas, and S. Godara, "Classification of Brain MRI Tumor Images: A Hybrid Approach," *Procedia Comput. Sci.*, vol. 122, pp. 510–517, 2017
- [5] S. Lu, Z. Lu, X. Hou, H. Cheng and S. Wang, "Detection of cerebral microbleeding based on deep convolutional neural network," 2017, *14th International Computer Conference on Wavelet Active Media Technology and Information Processing (ICCWAMTIP)*, Chengdu, 2017, pp. 93-96
- [6] M. H. O. Rashid, M. A. Mamun, M. A. Hossain and M. P. Uddin, "Brain Tumor Detection Using Anisotropic Filtering, SVM Classifier and Morphological Operation from MR Images," 2018, *International Conference on Computer, Communication, Chemical, Material and Electronic Engineering (ICAME2)*, Rajshahi, 2018, pp. 1-4
- [7] H. Mohsen, E.-S. A. El-Dahshan, E.-S. M. El-Horbaty, and A.-B. M. Salem, "Classification using deep learning neural networks for brain tumors," *Procedia Comput. Sci.*, vol. 3, no. 1, pp. 68–71, 2017. doi: 10.1016/j.fcij.2017.12.001
- [8] S. M. Kamrul Hasan and C. A. Linte, "A Modified U-Net Convolutional Network Featuring a Nearest-neighbor Re-sampling-based Elastic-Transformation for Brain Tissue Characterization and Segmentation," 2018, *IEEE Western New York Image and Signal Processing Workshop (WNYISPW)*, Rochester, NY, 2018, pp. 1-5.
- [9] S. T. Kebir and S. Mekaoui, "An Efficient Methodology of Brain Abnormalities Detection using CNN Deep Learning

- Network," 2018, *International Conference on Applied Smart Systems (ICASS)*, Medea, Algeria, 2018, pp. 1-5.
- [10] P. A. S. Deepak, "Brain tumor classification using deep CNN features via transfer learning", *Computers in Biology and Medicine*, vol. 111, 2019
- [11] P. Kumar Mallick, S. H. Ryu, S. K. Satapathy, S. Mishra, G. N. Nguyen and P. Tiwari, "Brain MRI Image Classification for Cancer Detection Using Deep Wavelet Autoencoder-Based Deep Neural Network," in *IEEE Access*, vol. 7, pp. 46278-46287, 2019
- [12] P. Liu, L. Zhao and Y. Ma, "Compressive sensing of multispectral image based on PCA and Bregman split," 2013, *IEEE International Geoscience and Remote Sensing Symposium - IGARSS*, Melbourne, VIC, 2013, pp. 2558-2561
- [13] C. J. Della Porta, A. A. Bekit, B. H. Lampe and C. Chang, "Hyperspectral Image Classification via Compressive Sensing," in *IEEE Transactions on Geoscience and Remote Sensing*
- [14] J. Cheng, «figshare. Dataset., » brain tumor dataset, 2 4 2017. [En línea]. Available: <https://doi.org/10.6084/m9.figshare.1512427.v5>. [Último acceso: 10 07 2019]
- [15] P. Arora, Deepali, and S. Varshney, "Analysis of K-Means and K-Medoids Algorithm for Big Data," *Procedia Comput. Sci.*, vol. 78, no.1, pp. 507–512, 2016
- [16] L. E. Mendoza. L. M. Meriño, "Compresión robusta usando compressive sensing (CS)", *Revista Colombiana de Tecnologías de Avanzada*, vol. 1, n° 33, 2019
- [17] A. S. Lundervold and A. Lundervold, "An overview of deep learning in medical imaging focusing on MRI," *Z. Med. Phys.*, vol. 29, no. 2, pp. 102–127, 2019
- [18] S. Zhang, L. Yao, A. Sun, and Y. Tay, "Deep learning based recommender system: A survey and new perspectives", *ACM Computing Surveys (CSUR)*, vol. 52, no. 1, pp. 1-38, 2019
- [19] S. Minaee, N. Kalchbrenner, E. Cambria, N. Nikzad, M. Chenaghlu and J. Gao, "Deep learning--based text classification: a comprehensive review", *ACM Computing Surveys (CSUR)*, vol. 54, no. 3, pp. 1-40, 2021
- [20] H. Ismail Fawaz, G. Forestier, J. Weber, L. Idoumghar, and P. A. Muller, "Deep learning for time series classification: a review", *Data mining and knowledge discovery*, 33(4), 917-963, 2019
- [21] P. Bharati and A. Pramanik, "Deep learning techniques—R-CNN to mask R-CNN: a survey", In *Computational Intelligence in Pattern Recognition* (pp. 657-668), 2020
- [22] S. Li, W. Song, L. Fang, Y. Chen, P. Ghamisi and J. A. Benediktsson, "Deep learning for hyperspectral image classification: An overview". *IEEE Transactions on Geoscience and Remote Sensing*, vol. 57, no. 9, pp. 6690-6709, 2019
- [23] A. Mikołajczyk and M. Grochowski, "Data augmentation for improving deep learning in image classification problem", In *2018 international interdisciplinary PhD workshop (IIPhDW)* (pp. 117-122). IEEE
- [24] X. Yang, Y. Ye, X. Li, X., R. Y. Lau, X. Zhang, and X. Huang, "Hyperspectral

- image classification with deep learning models". *IEEE Transactions on Geoscience and Remote Sensing*, vol. 56, no. 9, pp. 5408-5423, 2018
- [25] O. Stephen, M. Sain, U. J. Maduh, and D. U. Jeong, "An efficient deep learning approach to pneumonia classification in healthcare", *Journal of healthcare engineering*, 2019
- [26] M. Z. Hossain, F. Sohel, M. F. Shiratuddin and H. A. Laga, "Comprehensive survey of deep learning for image captioning", *ACM Computing Surveys (CSUR)*, vol. 51, no. 6, pp. 1-36, 2019
- [27] V. Antun, F. Renna, C. Poon, B. Adcock and A. C. Hansen, "On instabilities of deep learning in image reconstruction and the potential costs of AI", *Proceedings of the National Academy of Sciences*, vol. 117, no. 48, pp. 30088-30095, 2020
- [28] L. Jiao and J. Zhao, "A survey on the new generation of deep learning in image processing", *IEEE Access*, 7, 172231-172263, 2019
- [29] C. Tian, Y. Xu, L. Fei, and K. Yan, "Deep learning for image denoising: A survey". In *International Conference on Genetic and Evolutionary Computing* (pp. 563-572). Springer, Singapore, 2018
- [30] Z. Guo, X. Li, H. Huang, N. Guo, and Q. Li, "Deep learning-based image segmentation on multimodal medical imaging". *IEEE Transactions on Radiation and Plasma Medical Sciences*, vol. 3, no. 2, pp. 162-169, 2019
- [31] J. Dong, S. Roth and B. Schiele, "Deep wiener deconvolution: Wiener meets deep learning for image deblurring". *Advances in Neural Information Processing Systems*, vol. 33, pp. 1048-1059, 2020
- [32] C. Shorten, T. M. Khoshgoftaar and B. Furht, "Deep Learning applications for COVID-19", *Journal of big Data*, vol. 8, no. 1, pp. 1-54, 2021
- [33] S. Kuutti, R. Bowden, Y. Jin, P. Barber and S. Fallah, "A survey of deep learning applications to autonomous vehicle control", *IEEE Transactions on Intelligent Transportation Systems*, vol. 22, no. 2, pp. 712-733, 2020
- [34] O. Avcı, O. Abdeljaber, S. Kiranyaz, M. Hussein, M. Gabbouj and D. J. Inman, D. J. "A review of vibration-based damage detection in civil structures: From traditional methods to Machine Learning and Deep Learning applications", *Mechanical systems and signal processing*, vol. 147, pp. 107077, 2021
- [35] O. A. Montesinos-López, A. Montesinos-López, P. Pérez-Rodríguez, J. A. Barrón-López, J. W. Martini, S. B. Fajardo-Flores and J. & Crossa, "A review of deep learning applications for genomic selection", *BMC genomics*, vol. 22, no. 1, pp. 1-23, 2021
- [36] A. Esteva, K. Chou, S. Yeung, N. Naik, A. Madani, A. Mottaghi and R. Socher, "Deep learning-enabled medical computer vision", *NPJ digital medicine*, vol. 4, no. 1, 1-9, 2021
- [37] Y. Fu, Y. Lei, T. Wang, W. J. Curran, T. Liu and X. Yang, "Deep learning in medical image registration: a review", *Physics in Medicine & Biology*, vol. 65, no. 20, 20TR01, 2020
- [38] M. H. Hesamian, W. Jia, X. He and P. Kennedy, "Deep learning techniques for medical image segmentation: achievements and challenges", *Journal of digital imaging*, vol. 32, no. 4, 582-

596, 2019

- [39] J. Zhang, Y. Xie, Q. Wu and Y. Xia, "Medical image classification using synergic deep learning", *Medical image analysis*, vol. 54, pp. 10-19, 2019
- [40] S. K. Zhou, H. Greenspan, C. Davatzikos, J. S. Duncan, B. Van Ginneken, A. Madabhushi and R. M. Summers, "A review of deep learning in medical imaging: Imaging traits, technology trends, case studies with progress highlights, and future promises", *Proceedings of the IEEE*, vol. 109, no. 5, pp. 820-838, 2021
- [41] G. Currie, K. E. Hawk, E. Rohren, A. Vial and R. Klein, "Machine learning and deep learning in medical imaging: intelligent imaging", *Journal of medical imaging and radiation sciences*, vol. 50, no. 4, 477-487, 2019